EXPERIMENTAL CELL RESEARCH **234,** 249–258 (1997)
ARTICLE NO. EX973602

Characterization of Influenza Virus-Induced Death of J774.1 Macrophages

R. Joel Lowy[1] and Dimiter S. Dimitrov

Radiation Pathophysiology and Toxicology Department, Armed Forces Radiobiology Research Institute, Bethesda, Maryland 20889; and Section of Membrane Structure and Function, National Cancer Institute, National Institutes of Health, Bethesda, Maryland 20892

The mechanism and role of influenza virus (IV)-induced pathogenesis of macrophages during respiratory infection are ill defined. Reported here are findings on IV-induced cytopathic effects (CPEs) for an *in vitro* experimental system using the murine macrophage cell line J774.1. CPE was elicited by 0.2 or greater multiplicity of infection (m.o.i.). CPEs showed a lag of 6–8 h postinfection and occurred most rapidly between 6 and 12 h. J774.1 cells did not support productive IV replication, but immunofluorescence demonstrated that IV protein synthesis occurred. Light microscopy and DNA staining showed that after death cells had very condensed cytoplasm and nuclei. Cell remnants were surrounded by intact plasma membrane (PM) as demonstrated by exclusion of a membrane-impermeant dye. Time-lapse video microscopy recordings between 6 and 10 h postinfection showed sequential structural changes, including previously undescribed events. Notable changes were a rapid cytokinesis (zeiosis; "cell boiling"), followed by nuclear shrinkage, and an unusual transient blebbing of the PM. DNA fragmentation occurred after 12 h, producing a wide size range. UV-inactivated virus failed to induce CPEs, and CPE was blocked by amantadine. *N*-Acetylcysteine and pyrrolidine dithiocarbamate, but not other inhibitors of reactive oxygen intermediates, reduced or blocked the CPE. Most changes observed are those attributed to apoptotic processes rather than necrotic cell death. The kinetics and inhibitor effects suggest that IV infection and replication must be initiated to activate CPEs.

INTRODUCTION

Although influenza virus (IV) is one of the most extensively studied viruses and remains an important health problem, its pathogenesis at the cellular level is not completely understood. One important clinical aspect of IV infection is that it predisposes patients for subsequent upper respiratory bacterial infections, causing death in individuals whose immune systems are not robust [1–3]. The specific cellular and molecular mechanisms of this effect are still ill defined [2, 4], but previous work suggests that a contributing factor may be IV lesioning of macrophage function [4–8]. Consistent with this idea are observations in poultry showing that both lymphocytes and macrophages are destroyed during virulent influenza infections [9].

We report here initial findings on a convenient experimental system, using J774.1 cells, a well-characterized murine macrophage cell line, which allows study of cell biological, cell physiological, and immunological aspects of IV–macrophage pathobiology *in vitro*. Descriptions of IV-induced cell death have been reported for MDCK and HeLa cells [10], MDCK cells [11], an avian lymphocytic cell line [11], and human monocytes [12]. Based primarily on DNA fragmentation characteristics, as well as some cell structural and biochemical data, these authors concluded that cell death was occurring by apoptosis. The cell structural changes described here for the effect of IV on J774.1 cells were most similar to an apoptotic-like process and less consistent with necrosis [13, 14]. Time-lapse video microscopy demonstrated, for the first time, that the rapid extensive cytoplasmic fragmentation, the most dramatic and unique characteristic of apoptosis, is induced by IV in these macrophages. Previously undescribed changes for IV-induced pathogenesis include extensive vacuolization prior to this cytokinesis and the observation that the final nuclear and cytoplasmic condensation occurs later in the process. In contrast to previous reports of IV-induced cell death, DNA fragmentation occurs, but does not form "ladders" and is not an early marker of cell death. Also reported are results which show that J774.1 cell death does not occur with UV-inactivated virus or in the presence of the antiviral amantadine. Finally, thiol antioxidants, known to be effective blockers of cell death in other sytems, are shown to be effective against IV in these macrophages as well.

[1] To whom correspondence and reprint requests should be addressed at Radiation Pathophysiology and Toxicology Department, Armed Forces Radiobiology Research Institute, 8901 Wisconsin Avenue, Bethesda, MD 20889-5603. Fax: (301) 295-0313. E-mail: lowy@mx.afrri.usuhs.mil.

0014-4827/97

METHODS

Virus and cell culture. Concentrated stocks of IV strain X31 H3N2 were obtained as purified concentrates at 2 mg viral protein per milliliter (Specific Pathogen-Free Avian Supply, Preston, CT) and stored at −70°C. All plaque assays were performed using MDCK cells as described [15], but cultures were fixed with 4% formaline and stained with crystal violet. Virus titers are expressed as m.o.i. based on MDCK plaque-forming units per J774.1 cell, as J774.1 cells under these conditions did not support productive IV replication (see Results). The J774.1 macrophage cell line was maintained in spinner culture using RPMI 1640 medium supplemented with 10% heat-inactivated fetal bovine serum, 5000 U/ml each of penicillin and streptomycin, and 5 m*M* glutamine. MDCK cells were maintained in DMEM containing the same supplements. J774.1 cells were plated 24 h prior to use. Prior to exposure cells were transferred to a modified Hanks' basic saline glucose (HBSG) solution containing 10 m*M* Hepes and 4 m*M* bicarbonate at pH 7.3 and 5 m*M* glucose [16]. Concentrated virus was added to the cells, which were then incubated for 60 min at 37°C. Cells were then washed twice, returned to culture medium, and maintained for up to 48 h.

Microscopic morphological observation. Cells were plated either on 12-mm coverslips (Bellco Glass, Vineland, NJ) or in microculture chambers with a coverslip bottom (4 cm^2/chamber; No. 178565, Nunc, Napervile, IL) at 1×10^5 cells/cm^2 and exposed to virus. To examine the 24-h morphology cells were stained with 5–10 μg/ml Hoechst 33342 for 10 min and then examined by a digitally enhanced low-light-level fluorescence microscopy system using simultaneous differential interference contrast (DIC) optics and fluorescence [16]. To observe the effects of virus on live cells by DIC optics these same coverslip microculture chambers and exposure conditions were used. At 6 h postinfection cells were switched to HBSG, the HBSG was covered with mineral oil to reduce evaporation, and the chambers were mounted on a thermoelectrically heated custom stage which maintained the temperature at 37°C. DIC images of the same field of cells were recorded directly to video disc and video tape for later time-lapse analysis. Selected frames were photographed on 35-mm Panatonic-X film with a Polaroid freeze-frame system.

Immunofluorescence. Cells were fixed and stained as described by Martin and Helenius [17]. Briefly, cells were fixed in 4% fomaldehyde in neutral buffered PBS for 15 min at room temperature followed by 15 min in 50 m*M* NH_4Cl and permeabilized in 0.1% Triton X. The primary antibodies used for immunostaining were a clinical diagnostic monoclonal influenza A panel which included the H3N2 sera type (Bartel Diagnostic, Issaquah, WA), a commercially prepared polyclonal goat antibody to A/Texas/H3N2 (Virostat, Portland ME), and a X31 polyclonal rabbit antibody which has been previously described [18]. All secondary antibodies used were Fab fragments labeled with FITC and were, respectively, anti-mouse, donkey anti-goat, and donkey anti-rabbit. The secondary antibodies for use with the polyclonals were preabsorbed by the vendor to reduce most forms of cross species nonspecific staining ("min X ML"; Jackson Laboratories Immunological Laboratories, West Grove, PA). Preliminary experiments were performed with the polyclonal antibodies and the best staining levels with low background were obtained with the primary at 1:100 and the secondaries at 1:50. Preliminary experiments performed with noninfected or IV-infected cells stained with only the secondaries showed only nonspecific backgrounds equivalent to unstained cells. The best staining was obtained with the monoclonal and X31-specific polyclonal, which were nearly identical in their staining patterns. Cells were examined using a 100X 1.4 N.A. CF Fluor lens (Nikon, Melville, NY) and the fluorescent images were captured using a cooled camera system (Princeton Instruments, Trenton, NJ) and Metamorph image processing software (Universal Imaging Corp., West Chester, PA) and printed directly from digital image files using a dye-sublimation printer.

Cell viability. Cells were plated in 96-well plates at 1×10^5 cells per well. Twenty-four hours after infection cell survival was measured using a Cell Titer 96 AQueous kit (Promega, Madison, WI). This assay is a version of the commonly used MTT assay, but is based on the water-soluble MTS substrate. Preliminary experiments showed good sensitivity for cell numbers between 10^4 and 10^7 J774.1 cells. Experiments were also done using cells exposed to the vital dye nigrosin [19]. This dye is much easier to read than trypan blue and did not interfere with Hoechst fluorescence. Pharmacological treatments were added at the indicated concentrations to cells as a 2-h pretreatment, during the infection, and during the postinfection period. Due to interference between NAC and PDTC and the MTS reagent a MTT-based assay was used (Promega). Data are expressed as the percentage of unexposed controls without virus or pharmacological agents. Data for no virus but with drug exposure are also presented.

Quantitation of small nuclei formation. The observation that virus-exposed dying cells had much smaller nuclei was used to develop a semiautomatic method of quantification using fluorescence microscopy and image processing techniques (see Results). Cells were plated in 8-well microculture chambers (1 cm^2; No. 177402, Nunc) at 1×10^5 cell/cm^2 and infected at 4 m.o.i. Between 6 and 24 h the chambers were washed with HBS, fixed in 4% formaldehyde, and stained with Hoechst dye. For each treatment fluorescent images were recorded from a total of six regions, three from each of two replicated wells. Semiautomatic morphometric analysis of the nuclear sizes and numbers was performed using Image-1 software from Universal Imaging Corp. Preliminary experiments allowed size thresholds to be set such that nuclei were sorted into two size categories indicative of normal or small condensed nuclei. Preliminary experiments showed that thresholds could be set so that less than 10% of control cells were defined as condensed. For each treatment typically a total of between 100 and 400 nuclei were scored. The data are expressed as percentage small nuclei.

DNA fragmentation. J774.1 cells were plated in T-25 flasks at 2.50×10^6 cells. Exposures or sham infections were performed as described using 2 m.o.i. and harvested for DNA isolation between 0 and 48 h. CEM cells were incubated with an anti-Fas antibody (Q-Fas, UBI, Catalog No. 05-201) at 50 and 200 ng/ml for 24 h for use as a positive control. DNA was isolated using the Gentra Systems, Inc (Minneapolis, MN) kit. All cells were washed with PBS containing Ca^{2+} and Mg^{2+} and then lysed using 0.3 ml of the lysis buffer at room temperature. DNA is reported to be stable up to 1 year under these conditions. RNase A (2 μl, 1 mg/ml) was added and the mixture incubated for 1 h at 37°C. The protein precipitation solution (0.1 ml) was added, and the mixture was vortexed for 20 s and centrifuged for 3 min at 17,000g. The supernatant was poured into a clean 1.5-ml tube containing 0.3 ml 100% isopropanol and mixed. This was centrifuged for 1 min at 17,000g, the supernatant was removed, and the DNA pellet was washed with 70% ethanol. The DNA was hydrated in 0.1 ml TE. Electrophoresis was performed at 4°C with a 1% agarose gel that was stained with ethidium bromide. λ DNA–*Bst*E II digest was used as a marker of the fragment sizes. The samples were loaded on a 1.5% agarose gel and electrophoresed in 0.5% TBE buffer for 1 h at 5 V/cm. The DNA was stained with ethidium bromide and pictures were taken with a Polaroid camera.

RESULTS

Effect of virus titer on J774.1 survival. Figure 1 shows the effect of IV titer on J774.1 cell survival. Decreases in the number of cells occurred between 0.2 and 20 m.o.i. by 24 h. Virus stocks were UV exposed, a common method to inactive influenza, and its effects were confirmed by loss of plaque formation on MDCK

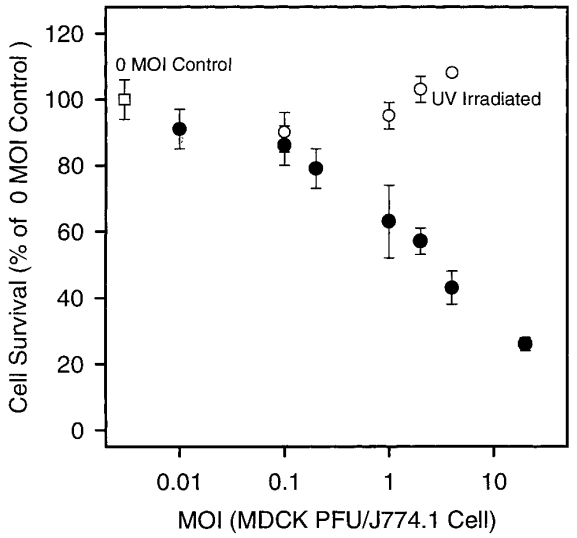

FIG. 1. Virus titer effect on cell number following IV exposure. Cells (1×10^5/well) in 96-well plates were exposed to varying titers of IV [note log scale and m.o.i. (multiplicity of infection) expressed as MDCK cell plaque-forming units per J774.1 cell. After 24 h cell survival was determined using the colorimetric MTS assay. Data are for cells exposed to live IV (solid circles), UV-inactivated IV (open circles) and mock exposed IV (open square). CPEs occur at titers above 0.2 m.o.i. for live IV. No CPE is observed for UV-treated IV. Data are expressed as means ± SEM for nine replicate cultures from three independent experiments. Data were calculated as percentage of paired mock-infected controls.

cells (data not shown). Inactivated virus failed to produce a CPE. This suggests that the macrophage response was not due to either a nonspecific effect, such as membrane damage by inactive virus particles, or cell signaling by influenza binding to macrophage surface receptors. Macrophages and monocytes have not been shown to support IV replication by most investigators, although production of low levels has been observed under some specialized culture conditions [4, 20, 21]. This was also true of the J774.1 cells. J774.1 cells in T-25 flasks were infected with 2 m.o.i. and showed the expected changes in morphology described below. Plaque assays conducted on MDCK cells using the medium from these J774.1 cells gave a PFU/ml of 2, approximately an 8 log reduction in titer from the viral stocks used to expose the J774.1 cells to virus. CPE assays were conducted at extended times up to 5 days postinfection (data not shown). At no m.o.i. was an increased CPE observed at later times. At intermediate m.o.i. after 48 h cell numbers began to return to initial levels due to replication of the surviving cells.

Immunofluorescence. Although permissive IV replication did not occur, the synthesis of IV proteins was supported by the J774.1 cells. Figure 2 shows light micrographs of J774.1 cells exposed to 4 m.o.i. and fixed at 6 h. This fixation time was chosen as being prior to loss of cells and cell structure during cell death, but at a time when influenza protein expression has been shown to reach a maximum in IV permissive cell lines. Cells exposed to virus show typical staining for IV, including both the nucleus and the cytoplasm (Figs. 2A and 2E). Only very low levels of combined autofluorescence and nonspecific immunostaining were observed for any of the 0 m.o.i. controls and are visible in part due to the sensitivity of the cooled CCD camera system (Figs. 2C and 2F). In two experiments a total of 200–400 cells were scored for each m.o.i. and the percentage

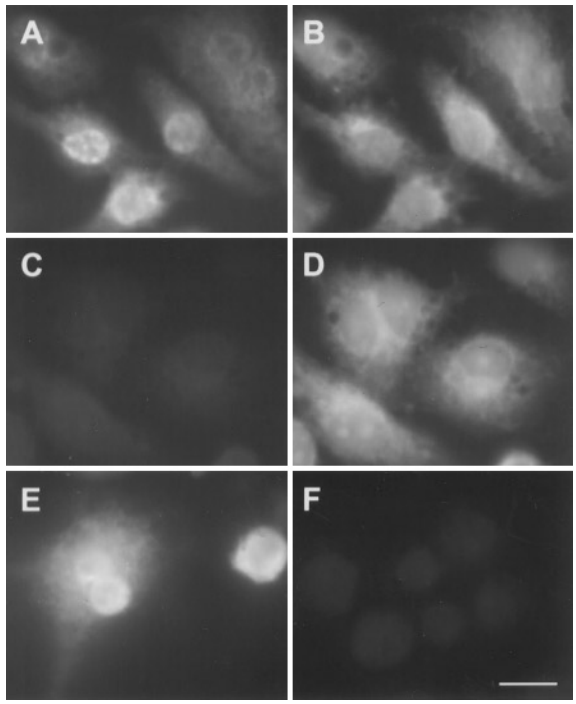

FIG. 2. Immunofluorescence staining of IV-exposed J774.1 cells. Cells were infected with 4 or 0 m.o.i., fixed, and stained as described at 6 h postinfection. The primary antibody was either a IV monoclonal panel of multiple sera types or a polyclonal to X31 followed by the appropriate FITC-labeled secondary antibody (see Methods). (A) 4 m.o.i. with monoclonal panel; (C) 0 m.o.i. with monoclonal panel. B and D are Evans blue counterstained red fluorescence to show cell locations for A and C, respectively. (E) 4 m.o.i. X31 polyclonal. (F) 0 m.o.i. X31 polyclonal. Cells infected with 4 m.o.i. show nuclear and cytoplasmic staining with the same pattern for both types of primary antibodies. Interestingly the cytoplasmic staining forms a fine net-like reticular structure in the J774.1 cells. Only low levels of autofluorescence/nonspecific staining occurred for the 0 m.o.i. controls, which is visible due to the high sensitivity of the low-light-level camera system. Fluorescent images in A, C, E, and F were acquired with FITC filters, and B and D were obtained with Texas red filters. No "cross-talk" between the filter sets was observed. All images were captured using a cooled CCD and image processing software (see Methods). Equivalent settings were used for the 4 and 0 m.o.i. treatments with each antibody so that intensities displayed are directly comparable. The polyclonal antibody resulted in slightly brighter staining, but all images were easily captured by the low-light-level camera system. Bar, 20 μm.

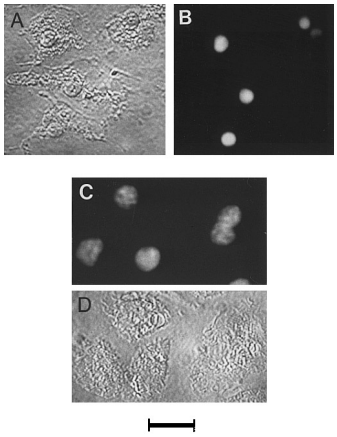

FIG. 3. Light microscopy appearance of IV-exposed and control cells. J774 cells were infected with 4 m.o.i. (A and B) or mock-infected (C and D) and fixed at 24 h. Cells were exposed to the membrane-impermeant dye nigrosin prior to fixation and to the DNA stain Hoechst 33323 afterward. Cells were examined by DIC (A and D) or fluorescence microscopy (B and C). IV-exposed cells have much smaller diameter nuclei which stain much more intensely and lose the heterogeneous staining pattern seen in the controls. The IV-exposed cells have distorted morphologies relative to those of controls and much more compact cytoplasm. In some cases the organelles are condensed to one side of the cell away from the plasma membrane. Despite these structural changes, IV-exposed cells, like control cells, do not have intense blue-black nuclear staining and therefore excluded the nigrosin dye. Bar, 5 μm.

of positive stained cells was determined. For input exposures of 0.1, 2, and 4 m.o.i. the respective percentages were 2, 56, and 88%. These data correlated well with the CPE values in Fig. 1.

Morphological changes. Morphological examination of cells postvirus exposure at 24 h (Figs. 3A and 3B) showed that the cells were very altered from the controls (Figs. 3C and 3D). They appeared smaller, but not detached or rounded, and had less cytoplasm. DIC microscopy showed the nuclei to be smaller and darker than normal. DNA staining with Hoechst dye (Figs. 3B and 3C) confirmed that the average nuclear size was reduced in diameter compared to the controls. DNA staining of normal J774.1 cells typically showed some chromatin structure (Fig. 3C) which is lost in virus-exposed cells. The staining intensity for these smaller nuclei was much greater than that of the controls by a factor of 200- to 300-fold. This difference is based on gain settings for the intensified camera system necessary to obtain images of a comparable gray-scale value which could be accurately recorded by the imaging system. Therefore despite being displayed at apparently similar intensities, the images were actually 2 logs different in intensity. It is unlikely that nuclear volume or thickness changes could readily account for this large change in DNA staining intensity; therefore an alteration in DNA condensation was the likely cause.

An important feature of differing forms of cell death is plasma membrane integrity. During necrosis there is cell swelling and rupture, leading to failure of the plasma membrane and extensive staining by dyes such as Trypan blue, nigrosin, and propidium iodide. In apoptotic processes these events do not occur or occur much later during a secondary phase of necrosis [14]. These differences in membrane permeablity have been used as the basis for flow cytometry assays of apoptotic cell death [22, 23]. The cells shown in Fig. 3 were exposed to nigrosin prior to fixation and Hoechst staining. Few floating cells were observed and care was taken to not lose cells from the substrate during dyeing, washing, and fixation. Although the nuclei appear darker in DIC due to their condensation, the intense blue-black staining expected for necrotic cells is not present. Figure 4 shows low-magnification light micrographs of cells exposed to virus at 4 (A) or 2 m.o.i. (B), or unexposed and permeabilized (C) with Triton X prior to staining with nigrosin and fixation. Only the Triton-X-treated cells show extensive staining. Even at 4 m.o.i., with extensive cell death and loss, as expected from the CPE measurement (Fig. 1), only a few of the remaining cells were stained.

Figure 5 shows that the kinetics of the formation of small nuclei (A) and CPE (B) up to 24 h postinfection had a very similar pattern. For both of these parameters the greatest change occurred after 6 h postinfection and by 12 h. A small increase in CPE (10–15%) by the MTS assay was measured prior to 8 h but was not likely to have been biologically significant (cf. standard error bars for 0 m.o.i. in Fig. 1). There was an additional increase in the number of cells showing small nuclei formation between 10 and 24 h, and a small additional decrease in cell viability measured between 12 and 24 h, but both of these changes were at a much slower rate. Interestingly these changes occur with a considerable lag, corresponding well to the 3- to 6-h lag in expression of IV proteins, but after 6 h the pathogenesis proceeds rapidly. Also, based on the 8-h time points, it appears the morphological changes slightly precede the metabolic marker. In contrast there was essentially no change for mock-infected cells. These kinetic data, as well as the titer data in Fig. 1, were generally consistent with those reported for a different strain of IV in human monocytes and a different macrophage cell line [24].

DNA fragmentation following viral exposure. The structural changes described above were indicative of cell death via an apoptotic mechanism (see Discussion). DNA fragmentation has been shown to occur in many cells undergoing apoptosis and is an important biochemical marker in most, but not all, cells [25, 26]. Figure 6 shows gels of DNA extracted from J774.1 cells mock infected (lanes 1–6) and infected at 2 m.o.i. (lanes

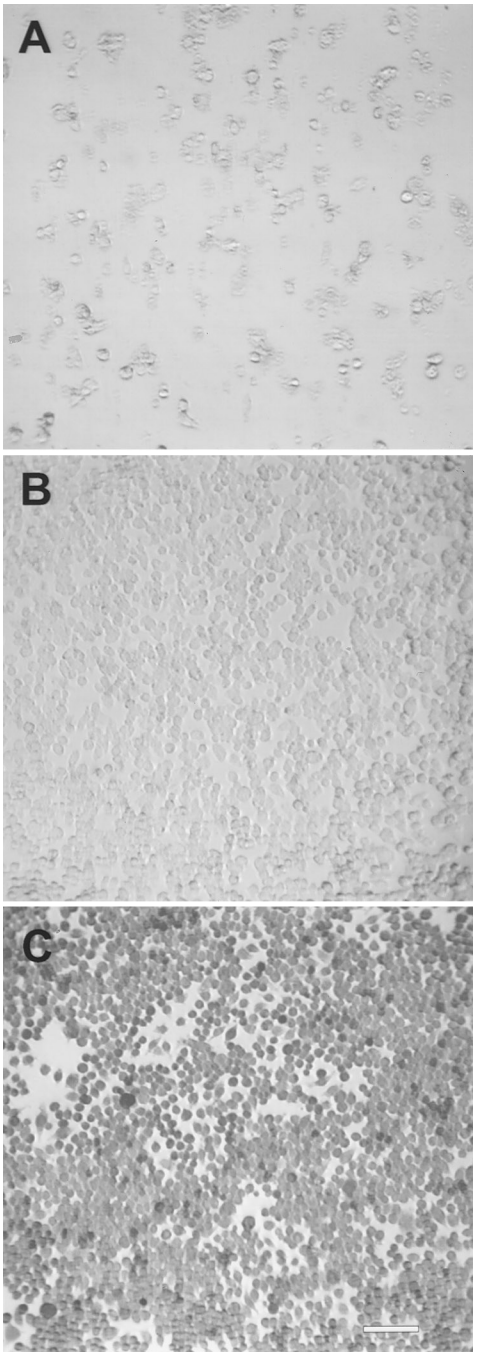

FIG. 4. Low-magnification light micrograph of nigrosin-exposed cells. Cells were infected with 4 m.o.i. (A), 2 m.o.i. (B), or mock-infected (C). At 24 h postinfection cells were exposed to nigrosin in PBS and fixed. Cells in C were permeabilized with 0.1% Triton X in PBS prior to nigrosin exposure. Low magnification allows the response to nigrosin of a large number of cells to be seen. All the permeabilized cells show typical blue-black staining, indicating plasma membrane permeability. In contrast few virus-exposed cells are positive at either m.o.i. Under these same conditions, measurements of cell survival (Fig. 1) indicated that at least 50% of the cells are dead. At 4 m.o.i. some nuclei have a darkened appearance and a loss of cells is evident. A few of these cells are positively stained, but most are condensed structures which appear slightly darker, as can be observed more clearly at higher magnification (Fig. 3). Bar, 100 μm.

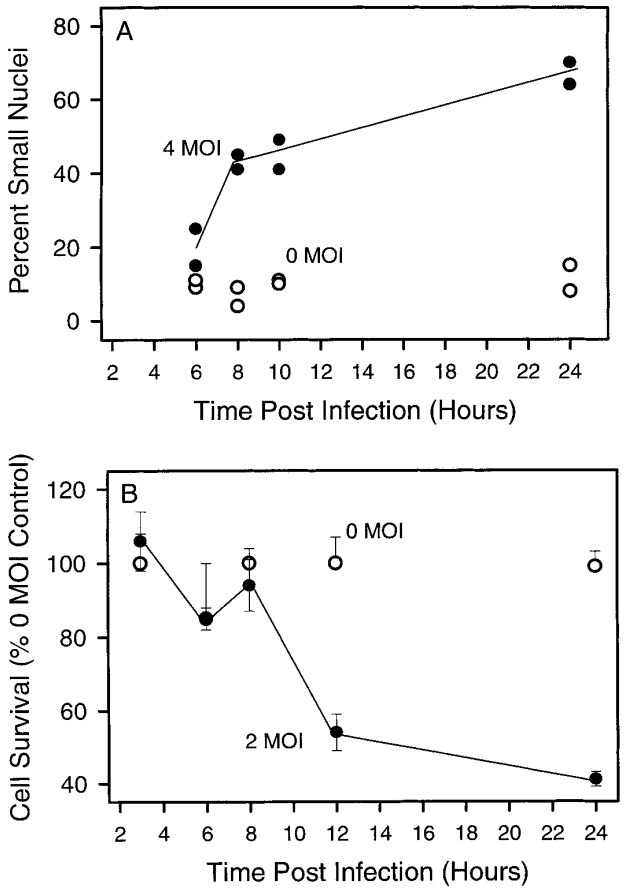

FIG. 5. Kinetics of CPE and small nuclei formation. In A cells were exposed to 4 m.o.i. in multiwell slide chambers. At 6, 8, 10, and 24 h postinfection cultures were fixed and the nuclei stained with Hoechst dye. Representative fields were examined using fluorescence video microscopy, and digital recording and a semiautomatic image processing algorithm were used to count and classify nuclei as either normal or condensed (see Methods) for exposed (closed circles) or mock-infected controls (open circles). The mean percentage of small nuclei is presented from two independent experiments. Few condensed nuclei were observed prior to 6 h postinfection but a rapid increase occurred by 8 h postinfection, which continued at a slower rate up to 24 h. No change in nuclear size was measured for mock-infected controls. In B cells were plated in 96-well plates and exposed to 0 or 2 m.o.i. and assayed for cell survival at the indicated times. Note change in abscissa from top panel. The pattern was similar to the formation of small nuclei. There was an initial lag of several hours prior to the greatest loss of cell viability between 8 and 12 h, with an additional but much smaller loss by 24 h. The decrease observed at 6 h postinfection was likely not to be biologically significant as a similar decrease was seen in the time-matched mock-infected cultures, and the cell survival value is within the variability seen for mock-infected cells (see Fig. 1). Data are means ± SEM for six cultures.

7–11) and harvested at 6–48 h. No DNA fragmentation was seen for the mock-infected cells or for the infected cells prior to 24 h. Fragmentation of the DNA was observed at 24 and 48 h, but cleavage created a broad range of sizes, not small base pair units. It is important

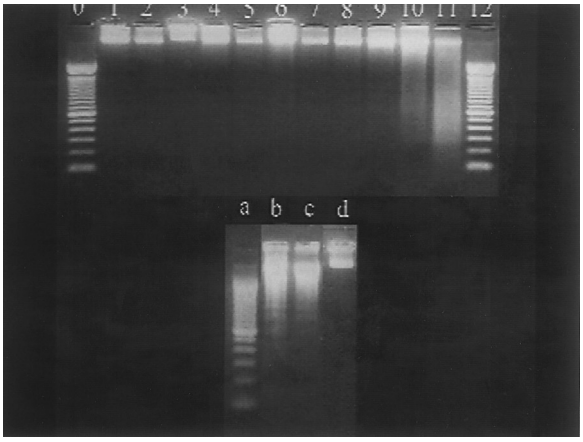

FIG. 6. Fragmentation of DNA. J774.1 cells were cultured in T-25 flasks and infected with 2 m.o.i. or mock-infected. At 0, 6, 8,12, 24, and 48 h postinfection medium was removed, and cells were gently washed once in PBS and treated with a cell-lysis DNA extraction buffer (see Methods). Lane 1 is 0 h mock-infected. Lanes 2–6 are mock-infected cells, and lanes 6–11 are IV-infected cells at 6, 8, 12, 24, and 48 h postinfection. Lanes 0 and 12 are molecular weight markers (λ DNA–*Bst*EII digest) of visible length between 224 and 8454. Only in the infected cells at 24 and 48 h was DNA fragmentation observed and without laddering characteristic of intranucleosomal fragmentation. Lanes a–b are DNA CEM cells exposed to anti-Fas antibody, which is known to induce apoptosis. Lanes are (a) molecular weight marker, (b) 200 ng/ml antibody, (c) 50 ng/ml antibody, and (d) untreated control. DNA laddering is seen in b and c.

to note that this DNA cleavage was not seen during the period of 6–12 h when the other markers for cell death are clearly evident.

As intranucleosomal cleavage yielding typical DNA ladders was not seen, these results were investigated further. Several alternate protocols for isolating DNA combined with different gel types and several DNA staining methods were used for analysis. These included extraction methods which removed most nonfragmented material and polyacrylamide gels stained with the very sensitive sybr green nucleic acid gel stain. All the results were similar to one another (data not shown). As a positive control the cell line CEM was exposed to an agent known to produce apoptosis, Anti-Fas antibody (Fig. 6, bottom, lanes a–d). The DNA from these cells was processed by the same methods used for the IV-exposed J774.1 cells. The CEM DNA, as expected, produced the characteristic small oligonucleotide laddering pattern generally associated with apoptosis.

In addition two different forms of *in situ* DNA nicked end labeling, e.g., "TUNEL" assays, from two differing manufacturers were used in an attempt to demonstrate intranucleosomal cleavage. In one case samples were submitted to the manufacturer for optimization of their protocol. In most case no labeling was seen at any viral titer level. In only one set of samples, 2 m.o.i. after 24 h, was any positive staining observed, but it was in less than 5% of the total cells.

Time-lapse observation of IV-induced cytopathic effect. Morphological criteria remain the most consistent markers for describing cell death processes and distinguishing between processes which are either primarily necrotic or apoptotic [27, 28]. Therefore it was important to describe morphological markers in more detail to better characterize the CPE in this experimental system. Of particular interest was whether the dramatic cytokinesis occurred (zeiosis, cell boiling), resulting in rapid cell fragmentation, which is considered an important and distinguishing characteristic of apoptotic processes [13, 14, 28]. Also, the well-defined limited time period IV induction of CPEs in the J774.1 cells combined with the availability of the imaging equipment provided an opportunity to obtain a more detailed continuous examination at the light microscopy level of virally induced cell death in a macrophage than has been previously reported to the best of our knowledge. Figure 7 shows single video frames, during the period of greatst change, for a cell that was observed continuously from 6 to 10 h postinfection at 4 m.o.i. The cell shown was taken from a larger field and is representative of changes observed for most of the other cells. An advantage of DIC optics, which uses heat-filtered white light, was that, unlike fluorescence measurements, these conditions were not damaging to the cells. Mitosis, a process sensitive to damaging conditions during microscopy, fortuitously occurred in one cell in the field (not shown) during the observation period. The displayed times are relative to the start of the recording, which was 6 h postinfection. The video frames selected are not evenly spaced so that the periods of greatest morphological change can be presented as a summary figure. The morphological changes included both changes previously described and new features not reported in earlier detailed descriptions of cell death processes, including those for virally induced CPEs [29–33].

The cells normally displayed small translational movements, accompanied by frequent retraction and extension of thin pseudopods (filopodia). The first morphological change was a flattening of the cell and loss of cytoplasmic extensions. The next change, which has not been previously described, was formation of large lucent vesicles in the cytoplasm and within the nuclear region. Many of these vesicles appeared to be apposed to both the inner and the outer surfaces of the nuclear membrane. There were very rapid changes in both the position and the size of these vesicles. In some cells this process stopped, the cells partially returned to a more rounded appearance, and cytoplasmic extensions reappeared. These cells then reflattened and repeated the lucent vesicle

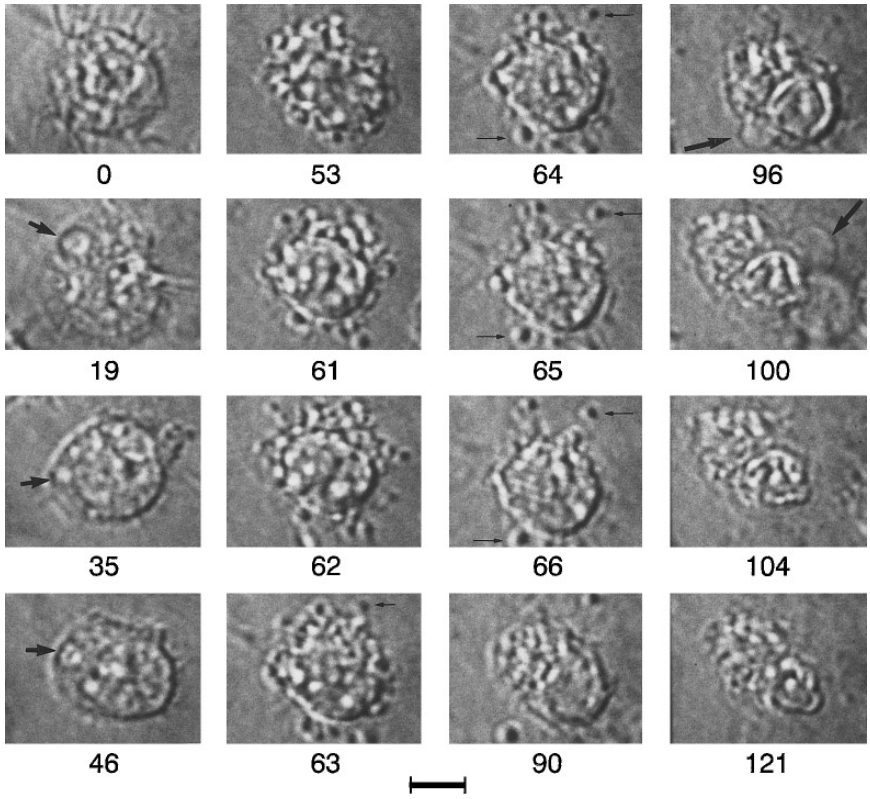

FIG. 7. DIC images from time-lapse video microscopy. J774.1 cells were exposed to 4 m.o.i. At 6 h postinfection exposed cells were mounted on the microscope in a temperature-regulated chamber at 37°C. DIC images were recorded continuously at low light levels using heat-filtered white light between 6 and 10 h postinfection. Images for a single cell, illustrating typical morphological changes, are shown. Times points shown, labeled on each panel, were selected for periods of greatest change and are relative to 6 h postinfection which is equal to record time 0. Times 0 to 35 min illustrate the initial cell flattening, loss of filopodia, and rapid formation of large lucent cytoplasmic vesicles (arrowhead). Times 61 to 66 min show the cytoplasmic boiling or zeiosis and release of small vesicles or organelles (arrows). Times 96 to 121 min show the formation and subsequent retraction of membrane blebs (arrows) and the final cytoplasmic and nuclear shrinkage, terminating in an apoptotic body. Bar, 5 μm.

formation sequence. Further observation is needed to resolve whether these are changes in the nuclear membrane, apposition of intracellular compartments, or the formation of macropinosomes [34] from the cell surface. If internal, these vesicles may be a feature of regulated J774.1 cell death. There is a single report showing electron micrographs of what may be similar lucent vesicles during cell death induction by a very different agent, cytotoxic lymphocytes [35].

In the next stage for all cells the cytoplasm took on a very granular appearance, with the formation of small phase-bright and phase-dark structures, which also displayed rapid movements. In some cells these could be seen as small vesicles that rapidly budded off from the cell surface. This rapid cytokinesis (zeiosis) was well described as a boiling appearance in previous reports (see Discussion). Upon the appearance of these small rapidly moving vesicles, the cytoplasmic region, but not the nuclear region, appeared to decrease in area. Next, as the small vesicle formation and budding decreased in frequency, the cytoplasmic area appeared to become larger in proportion while the nucleus began to decrease in size. In some cells the cytoplasmic area did not seem to expand much but became a larger portion of the cell profile due to the decrease in the nucleus. During the period that the nuclear profile continued to decrease, one or more large expansions, or blebs, of the plasma membrane generally occurred. These previously undescribed blebs were composed of very clear membrane-bound cytoplasm and appeared to contain no organelles. These plasma membrane blebs did not rupture but shrank until they either disappeared or formed a small organelle-free region to one side of the cell. A possible cause may be loss of cytoskeletal anchor elements at localized sites and/or transient loss of ion and water homeostasis. As the membrane swelling was not permanent, the cells must generally regain volume regulation and ion–water homeostasis. During this period there appeared to be additional shrinkage of both the nucleus and the cytoplasm-containing organelles.

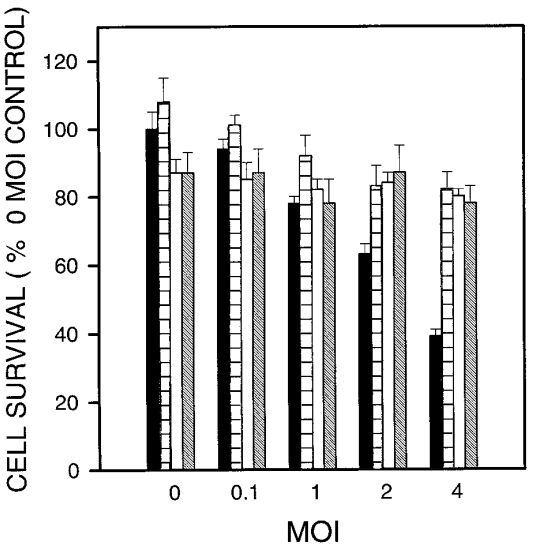

FIG. 8. Effect of amantadine on IV-induced CPE. J774.1 cells were infected with the indicated titers of virus or mock-infected. Amantadine was added to both mock-infected and infected cells as a 2-h pretreatment, during the infection, and during the 24-h postinfection culture period. Amantadine concentrations were 0 μg/ml (solid bars), 5 μg/ml (horizontally striped bars), 15 μg/ml (open), and 25 μg/ml (cross hatched). At 1, 2, and 4 m.o.i. all concentrations of amantadine reduced the CPE to control levels. Amantadine did show a small CPE at 15 and 25 μg/ml. Data are means ± SEM for six cultures from two independent experiments.

Both the membrane swelling and the cytoplasmic contraction are consistent with the possibility of a large transient calcium influx. Once the membrane bleb decreased, no further changes were evident. The final cell appearance was identical to that of the small cell remnants, apoptotic bodies, observed in the other cytopathic experiments (Fig. 3).

Effects of amantadine on CPE. The results with UV-inactivated virus suggested that the CPEs of the J774.1 cells required infection by IV, not merely surface binding. The effects of amantadine on IV have been extensively studied and the blockage for most IV strains occurs during entry via the endocytic pathway with even the earliest IV replication events being inhibited. For details and review of the molecular basis of amantadine's effects see Ref. [36]. Figure 8 shows that, as expected, 5 μg/ml blocked CPEs in the J774.1 cells. Higher concentrations did not reduce the virally induced CPEs further, but were slightly cytopathic to the controls. Amantadine added between 1 and 6 h postinfection, as expected for the X31 IV strain, did not block CPEs (data not shown).

Effect of antioxidants. Antioxidants have been shown to block apoptosis, including virus-induced CPE in a wide number of experimental systems, including influenza virus *in vivo* [37]. Among the mechanisms for ROIs activating cell death, in both viral and nonviral systems, that have been suggested are nonspecific cellular damage, cell signaling agents that activate transactivation factors [38], and most recently mitochondrial proteins that activate proteases associated with apoptosis [39]. Figure 9 shows the effect of several different types of ROI inhibitors. Only the thiol agents NAC and PDTC were effective in blocking the IV-induced CPEs, while the other antioxidants, desferoximine nesyiate, a metal chelator, trolox, a peroxidation inhibitor, and catalase, a hydrogen peroxide inhibitor, were ineffective.

DISCUSSION

These studies describe several important observations concerning IV-induced death of J774.1 macrophages. Data are presented on the virus titers needed for CPE and kinetics of this particular experimental system. The data for UV-treated virus, CPE kinetics, and amantadine all support the idea that infection and IV replication are necessary to activate CPE. CPE does not appear to be due to either cell surface-mediated signaling events or nonspecific cell membrane damage. These results confirm and extend the observation that cyclohexamide blocked IV-induced apoptosis in MDCK cells [10].

Determining the likely mechanism of virally induced

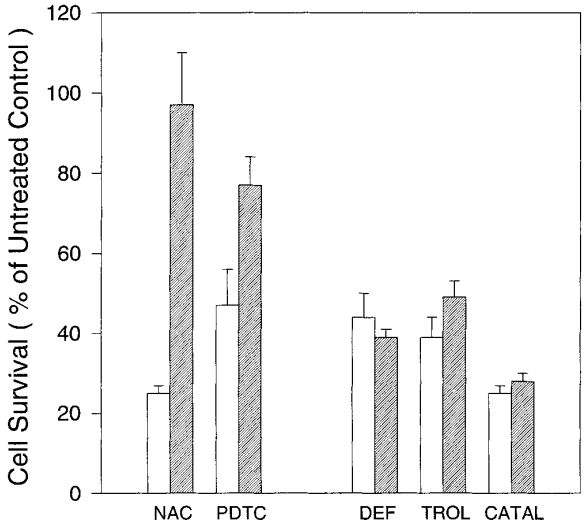

FIG. 9. Effect of antioxidants on IV-induced CPE. J774.1 cells were infected with 4 m.o.i. in the absence (white bars) or in the presence of various agents (shaded bars) and the cell survival was assayed. Inhibitors were *N*-acetylcysteine (NAC, 50 m*M*), pyrrolidine dithiocarbamate (PDTC, 100 m*M*), deferoximine nesyiate (DEF, 0.5 m*M*), trolox (TROL, 1.0 m*M*), and catalase (5000 U/ml). Only the two thiol antioxidants were effective in blocking the IV-induced CPE. Data are means ± SEM for six cultures from two independent experiments performed for each drug. Data are normalized to untreated mock-infected cultures performed as controls with each drug (values not shown).

cell death is of considerable interest for many virus–host cell interactions, with apoptosis often being favored over necrosis [40]. Morphological characteristics of the apoptotic process include nuclear, cytoplasmic, and plasma membrane shrinkage, chromatin condensation, lack of plasma membrane rupture, and cytokinesis by rapid blebbing (zeiosis). Necrotic processes differ by producing cytoplasmic swelling, cell rupture, and failure of the plasma membrane, but no change in nuclear morphology and no cytokinesis. DNA fragmentation occurs in most but not all apoptotic systems, and there are increasing reports that classic laddering is not always observed. Intranucleosomal cleavage associated with apoptosis can result in formation of small fragments, larger oligomers, or both [25, 26, 41]. Recent methodological reviews caution that morphological changes are still the best criterion for distinguishing apoptosis from necrosis [27, 28]. Despite the importance of IV pathogenesis, there are few studies relative to other viral types [40]. Two studies reported apoptosis in MDCK cells, an epithelial cell line which supports IV replication [10, 11]. In one of these reports apoptosis was also observed in RP9 cells, an avian lymphocyte line [11]. To date there has been only one brief report demonstrating that IV causes apoptosis in cells of the macrophage/monocyte lineage [12] based on morphology and DNA fragmentation. It was expected that CPE in J774.1 cells would show similar characteristics, consistent with apoptotic cell death. The morphological observations for J774.1 cells correspond well to both brief descriptions of apoptotic structural changes for IV-induced apoptosis and the more detailed descriptions from other experimental systems [13, 14, 26]. This conclusion is based on direct comparisons between images of the J774.1 cell structural changes and final cell remnant morphologies with descriptions and pictures of apoptotic processes in previous reports [29, 31–33]. Importantly the J774.1 cells underwent both nuclear and cytoplasmic shrinkage and the latter occurred by the characteristic dramatic vesicularization and budding of the cytoplasm, i.e., zeiosis or cell boiling (Fig. 7) [29, 31–33]. The nuclear changes occurred after cytokinesis. Typical necrotic markers, such as cell rupture or maintenance of intact nuclear morphology, were not observed. There was no loss of J774.1 membrane integrity (Figs. 3 and 4), which contrasted the descriptions of IV-induced CPEs in human monocytes [42]. However, the DNA cleavage pattern seen in this study was not that typically expected of apoptotic systems. The cleavage which did occur was not kinetically well coordinated with the other cytopathic changes, suggesting that it was a later secondary process. This lack of typical laddering was surprising, as bacterial toxins have been shown to induce laddering in J774.1 cells, although their appearance is not as sharply defined as those reported for lymphoid cells [43, 44]. However, several reports of apoptosis in macrophages also failed to observe typical DNA laddering [45], including J774.1 cells [46]. The reasons for differences in this or any other system, particularly relative to the clear laddering generally observed in T-cells, are still obscure [25]. Currently the only alternatives for classification of cell death are as necrotic or apoptotic. All of the observations made in this study, except for DNA fragmentation, are consistent with apoptosis and not with necrosis. Therefore it seems likely that IV induces a regulated form of cell death in the J774.1 cells as well, which is best described as an apoptotic-like process. Finally, the order of these structural changes may be important in understanding underlying biochemical events. In this system it is clear that nuclear condensation is a late and terminal event and is preceded by cytokinesis. The causal relationship between nuclear changes and the other events during CPE, such as zeiosis, bears further investigation.

The mechanism of IV-induced cell death, as for all viruses to date, is still not completely defined. Broadly possibilities include (a) nonspecific cell damage, such as changes in membrane permeability; (b) relatively nonspecific biochemical mechanisms due to a general down-regulation of host protein synthesis; (c) specific IV interference with regulators of cell death; and (d) autocrine effects of either ROI or cytokines. Each of these possibilities warrants investigation. However, if relatively nonspecific mechanisms, such as protein synthesis inhibition, dominate, it is surprising that antioxidants were effective in blocking cell death. Furthermore the result that only the thiol antioxidants were effective suggests that specific IV–cell interactions are occurring and can be manipulated. If ROIs were acting only as cell damaging agents, then the other antioxidants should have blocked the CPE. A suggestion for IV–host cell signaling pathways leading to apoptosis has been made based on transfection and expression of IV HA, leading to activation of NF-κ B [47]. It was postulated that this could be the mechanism for IV-induced apoptosis and that modulation with antioxidants which block NF-κB should be effective in blocking apoptosis. However, their results and those presented here are in contrast to results obtained with MDCK cells in which antioxidants failed to block the CPE [48]. Also further investigation of an autocrine role for cytokines is warranted. IV has been shown to elicit TNF-α, IL1-β, and IL-6 [20, 24, 49]. J774.1 cells, like other macrophage/monocyte cells, produce or respond to a variety of immunomodulators [46, 50–53], including secretion of TNF-α [54], an important immune system inducer of cell death.

In conclusion, J774.1 cells are readily maintained in culture, easily obtained in large numbers, and have many characteristics of *in vivo* macrophages, including the ability to produce various immunomodulators. Therefore, the IV–J774.1 cell system described here is likely to provide an additional valuable experimental system for studying IV–macrophage interactions including cell death and aid in our understanding of IV-induced pathogenesis.

The collegiality, help, and useful discussions of Drs. Robert Blumenthal, Anu Puri, Charles Pak, and Gary Whittaker are gratefully acknowledged. The gift of the X31 polyclonal antibody from Dr. Ari Helenius is also gratefully acknowledged. Support was through NIAID Grant AI 35892 to R.J.L.

REFERENCES

1. Abramson, J. S., and Mills, E. L. (1988) *Rev. Infect. Dis.* **10,** 326–341.
2. Murphy, B. R., and Webster, R. G. (1990) *in* Virology (Fields, B. N., and Knipe, D. M., Eds.), 2nd ed., pp. 1091–1152, Raven Press, New York.
3. White, D. O., and Fenner, F. J. (Eds.) (1994) Medical Virology, 4th ed., pp. 1–603, Academic Press, New York.
4. Sweet, C., and Smith, H. (1980) *Microbiol. Rev.* **44,** 303–330.
5. Astry, C. L., and Jakab, G. J. (1984) *J. Virol.* **50,** 287–292.
6. Laegreid, W. W., Liggitt, H. D., Silflow, R. M., Evermann, J. R., Taylor, S. M., and Leid, R. W. (1989) *J. Leukocyte Biol.* **45,** 293–300.
7. Morgensen, S. (1979) *Microbiol. Rev* **43,** 1–26.
8. Rouse, B. T., and Horohov, D. W. (1986) *Rev. Infect. Dis.* **8,** 850–873.
9. Van Campen, H., Easterday, B. C., and Hinshaw, V. S. (1989) *J. Gen. Virol.* **70,** 2887–2895.
10. Takizawa, T., Matsukawa, S., Higuchi, Y., Nakamuara, S., Nakanishi, Y., and Fukuda, R. (1993) *J. Gen. Virol.* **74,** 2347–2355.
11. Hinshaw, V. S., Olsen, C. W., Dybdahl-Sissoko, N., and Evans, D. (1994) *J. Virol.* **68,** 3667–3673.
12. Fesq, H., Bacher, M., Nain, M., and Gemsa, D. (1994) *Immunobiology* **190,** 175–182.
13. Duvall, E., and Wyllie, A. H. (1986) *Immunol. Today* **7,** 115–119.
14. Wyllie, A. H., Kerr, J. F. R., and Currie, A. R. (1980) *Int. Rev. Cytol.* **68,** 251–306.
15. Patterson, R. G., and Lamb, R. A. (1993) *in* Molecular Virology A Practical Approach (Davison, A. J., and Elliott, R. M., Eds.), 1st ed., pp. 35–72, IRL Press, New York.
16. Lowy, R. J., Sarkar, D. P., Whitnall, M. H., and Blumenthal, R. (1995) *Exp. Cell Res.* **216,** 411–421.
17. Martin, K., and Helenius, A. (1991) *Cell* **67,** 117–130.
18. Braakman, I., Hoover-Lity, H., Wagner, K. R., and Helenius, A. (1992) *J. Cell. Biol.* **114,** 401–411.
19. Katenbach, J. P., Katenbach, M. H., and Lyons, W. B. (1958) *Exp. Cell Res.* **15,** 112–117.
20. Bender, A., Amann, U., Jager, R., Nain, M., and Gemsa, D. (1993) *J. Immunol.* **151,** 5416–5424.
21. Rodgers, B., and Mims, C. A. (1981) *Infect. Immun.* **31,** 751–757.
22. Dive, C., Gregory, C. D., Phipps, D. J., Evans, D. L., Milner, A. E., and Wyllie, A. H. (1992) *Biochim. Biophys. Acta* **1133,** 275–285.
23. Belloc, F., Dumain, P., Boisseau, M. R., Jalloustre, C., Reiffers, J., Bernard, P., and Lancone, F. (1994) *Cytometry* **17,** 59–65.
24. Nain, M., Hinder, F., Gong, J.-H., Schmidt, A., Bender, A., Sprenger, H., and Gemsa, D. (1990) *J. Immunol.* **145,** 1921–1928.
25. Bortner, C. D., Oldenburg, N. B. E., and Cidlowski, J. A. (1995) *Trends Cell Biol.* **5,** 21–26.
26. Martin, S. J., Green, D. R., and Cotter, T. G. (1994) *Trends Biochem. Sci.* **19,** 26–30.
27. Eastman, A. (1995) *Methods Cell Biol.* **45,** 41–55.
28. Kerr, J. F., Golbe, G. C., Winterford, C. M., and Harmon, B. V. (1995) *Methods Cell Biol.* **46,** 1–27.
29. Hurwitz, C., and Tolmach, L. J. (1969) *Biophys. J.* **9,** 607–633.
30. Knipe, D. M. (1990) *in* Virology (Fields, B. N., and Knipe, D. M., Eds.), 2nd ed., pp. 293–314, Raven Press, New York.
31. Laster, S. M., Wood, J. G., and Gooding, L. R. (1988) *J. Immunol.* **141,** 2629–2634.
32. Mullinger, A. M., and Johnson, R. T. (1976) *J. Cell. Sci.* **22,** 242–285.
33. Sanderson, C. J. (1976) *Proc. R. Soc. London B* **192,** 241–255.
34. Alpuche-Aranda, C. M., Racoosin, E. L., Swanson, J. A., and Miller, S. I. (1994) *J. Exp. Med.* **179,** 601–608.
35. Shibata, S., Kyuwa, S., Lee, S.-K., Toyoda, Y., and Goto, N. (1994) *J. Virol.* **68,** 7540–7545.
36. Lamb, R. A., and Krug, R. M. (1996) *in* Virology (Fields, B. N., Howley, P. M., and Knipe, D. M., Eds.), 2nd ed., pp. 1353–1396, Lippincott-Raven, New York.
37. Schwarz, K. B. (1996) *Free Radical Biol. Med.* **21**(5), 641–649.
38. Lin, K.-I., Lee, S.-H., Narayanan, R., Baraban, J. M., Hardwick, J. M., and Ratan, R. R. (1995) *J. Cell. Biol.* **131,** 1149–1161.
39. Kroemer, G., Zamzami, N., and Susin, S. A. (1997) *Immunol. Today* **18,** 44–51.
40. Razvi, E. S., and Welsh, R. M. (1995) *Adv. Virus Res.* **45,** 1–60.
41. Oberhammer, F., Wilson, J. W., Dive, C., Morris, I. D., Hickman, J. A., Wakerling, A. E., Walder, P. R., and Sikorska, M. (1993) *EMBO J.* **12,** 3679–3684.
42. Pescheke, T., Bender, A., Nain, M., and Gemsa, D. (1993) *Immunobiology* **189,** 340–355.
43. Khelef, N., Zychlinsky, A., and Guiso, N. (1993) *Infect. Immun.* **61,** 4064–4071.
44. Zychlinsky, A., Prevost, M. C., and Sansonetti, P. J. (1992) *Nature* **358,** 167–169.
45. Munn, D. H., Beall, A. C., Song, D., Wrenn, R. W., and Throckmorton, D. C. (1995) *J. Exp. Med.* **181,** 127–136.
46. Fujihara, M., Ito, N., Pace, J. L., Watanabe, Y., Russell, S. W., and Suzuki, T. (1994) *J. Biol. Chem.* **269,** 12773–12778.
47. Pahl, H. L., and Baeuerle, P. A. (1995) *J. Virol.* **69,** 1480–1484.
48. Olsen, C. W., Dybdahl-Sissoko, N., and Hinshaw, V. S. (1996) *Death Differ.* **3,** 191–197.
49. Sprenger, H., Bacher, M., Rischkowsky, E., Bender, A., Nain, M., and Gemsa, G. (1994) *J. Immunol.* **152,** 280–288.
50. Chen, B. D.-M., and Lin, H.-S. (1984) *J. Immunol.* **132,** 2955–2960.
51. Miyakawa, Y., Kagaya, K., Watanabe, K., and Fukazawa, Y. (1995) *Microbiol. Immunol.* **33,** 1027–1038.
52. Salo, R. J., Bleam, D. K., Greer, V. L., and Ortega, A. P. (1985) *J. Leukocyte Biol.* **37,** 395–406.
53. Tosk, J., Lau, B. H. S., Myers, R. C., and Torrey, R. R. (1989) *J. Leukocyte Biol.* **46,** 103–108.
54. Sakurai, A., Satomi, N., and Haranaka, K. (1985) *Cancer Immunol. Immunother.* **20,** 6–10.

Received November 22, 1996
Revised version received March 5, 1997